

# Quantifying Variability in the Planum Temporale: A Probability Map

C.F. Westbury, R.J. Zatorre and A.C. Evans<sup>1</sup>

Department of Neuropsychology and Cognitive Neuroscience and <sup>1</sup>McConnell Brain Imaging Centre, Montreal Neurological Institute and Hospital, Montreal, Quebec, Canada

The acquisition of definitive evidence for systematic hemispheric asymmetries in the size of the planum temporale (PT) has been restricted by difficulties in identifying, standardizing and measuring the region of interest. In this paper an operational definition for identifying the problematic posterior border of the PT on magnetic resonance imaging (MRI) scans is proposed. An interactive voxel-painting program was used to identify and label the PT simultaneously in horizontal, sagittal and coronal planes in MRI scans, transformed into the standardized Talairach–Tournoux stereotaxic space, from 50 normal right-handed volunteers. Both grey matter volume and cortical surface area of the PT were measured, while controlling for individual variation in overall brain shape and volume. The labeled tissue was averaged together to produce a probability map in standardized space of the region of interest. The PT region is highly variable, with no single voxel being labeled with a probability of >65%. In this study there were no significant hemispheric differences in volume or area of the PT. An asymmetry in area and volume was introduced by using an alternative method – the ‘knife-cut’ method – for identifying the posterior border. Implications for functional neuroimaging of the PT are discussed.

## Introduction

The planum temporale (PT) is the undulating surface of the superior temporal gyrus posterior to Heschl’s gyrus. Although the PT has been described as exhibiting ‘the best-defined asymmetries in the gross configuration of the human cerebral cortex’ (Galaburda *et al.*, 1978), it has also been noted that ‘the macroanatomic boundaries of the PT cannot always be determined with certainty’ (Steinmetz *et al.*, 1989). The uncertainty regarding the borders of the PT is reflected in the fact that planimetric estimates of the average left PT surface area, using ostensibly identical definitions for identifying the boundaries, have varied by over 300%, from 562 mm<sup>2</sup> (Kulynych *et al.*, 1993) to 1931 mm<sup>2</sup> (Karbe *et al.*, 1993). Comparisons between studies are further complicated by the claim (Wada *et al.*, 1975) that up to 10% of brains have no right PT at all. The variability in the literature on PT asymmetry springs mainly from the difficulty of providing an unambiguous operational definition for identifying the problematical posterior border. In this paper we used operationalized definitions of the borders of the PT, in order to define a probabilistic map of the PT in the standardized Talairach–Tournoux stereotaxic space (Talairach and Tournoux, 1988), which we propose may serve a role in assessing future claims of functional asymmetry in this region of the brain.

## An Operational Definition of the PT

The development of an operational definition of the PT is a necessary step in constructing a probability map. Not only has there been much uncertainty about how to reliably identify the borders of the PT in all cases, but [as Steinmetz pointed out (Steinmetz, 1990)] the anatomical criteria by which the PT was identified were not precisely described in most early studies of

the PT (Geschwind and Levitsky, 1968; Tezner *et al.*, 1972; Witelson and Paallie, 1973; Wada *et al.*, 1975; Bossy *et al.*, 1976; Chi *et al.*, 1977; Kopp *et al.*, 1977; Falzi *et al.*, 1982; Pieniadz and Naeser, 1984; Galaburda *et al.*, 1987).

The mesial and anterior borders of the PT are clearly and uncontroversially defined. The mesial border is the point where the PT fades into the insula. The anterior border is marked [using Pfeifer’s criterion (Pfeifer, 1936)] by the sulcus lying behind Heschl’s gyrus, or behind the first gyrus if there is more than one, since it is known that the primary auditory cortex is primarily on the most anterior gyrus (Rademacher *et al.*, 1993). When no Heschl’s gyrus is visible, because it does not extend all the way to the lateral edge of the Sylvian plane, the anterior border is marked by the extension of the first gyrus to the lateral edge.

The posterior border of the PT has traditionally been defined by the application of the ‘knife-cut’ rule, which determines the posterior border of the PT in brains scans by imagining a projection continuing the planar surface of the temporal lobe onto the posterior surface, or, in anatomical specimens, by actually cutting along that plane with a dissecting knife. The knife-cut method has been applied with good inter-rater reliability within individual research groups (Kulynych *et al.*, 1993, 1994). However, the large variability of area estimates obtained between different research groups using the method suggests that it has not been well defined operationally, making it difficult to assess how it was applied in any individual study.

The blind application of the knife-cut rule in the sagittal plane, as has been done in some magnetic resonance imaging (MRI)-based studies, cannot always exclude homologous tissue in all cases. The reason for this can be seen by a consideration of the four main types of cases which are encountered. These are illustrated in cartoon form in Figure 1.

The simplest and least controversial case (Fig. 1A) is the one in which all the relevant landmarks are clear. The three characteristics that define such cases are: (i) a clear Heschl’s gyrus, marking the anterior border of the PT; (ii) the existence of the roughly planar Sylvian surface [Witelson *et al.*’s horizontal planum temporale, or HPT (Witelson *et al.*, 1995)]; and (iii) the existence of unambiguous ascending and descending rami of nearly equal lengths, forming a rough ‘Y’ shape (tipped posteriorly) at the end of the Sylvian fissure.

In keeping with terminology introduced by Witelson and Kigar (Witelson and Kigar, 1992), we will refer to cases that meet these three criteria as H&V-type PTs. An example of an H&V-type PT is shown in Figure 2.

In one simple variation of the H&V-type PT, the ascending ramus is much longer than the descending ramus (see Fig. 1B). In such cases, there is an asymmetry at the posterior end of HPT, with the ‘Y’ shape which is formed by the ascending and descending rami in the H&V-type PT being distorted by

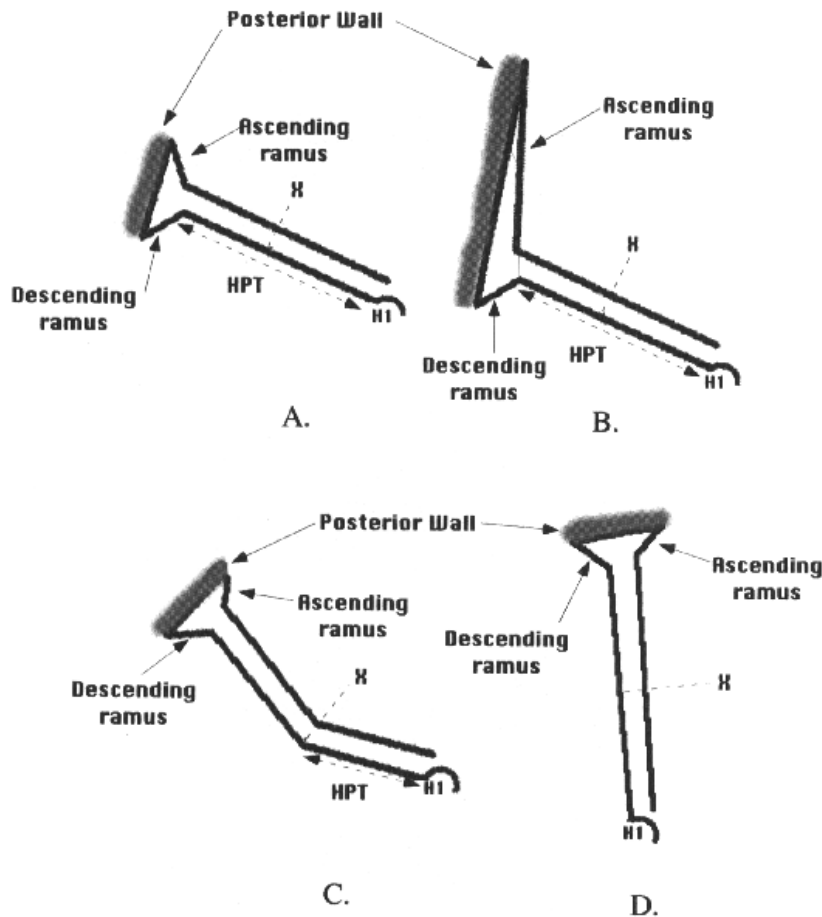


**Figure 1.** Schematic illustrations of four types of PT. Each diagram represents a cartoon of the Sylvian fissure viewed in sagittal section (anterior to the right, posterior to the left), from Heschl's gyrus (H1) back to the posterior wall (shaded). Four different configurations are shown of ascending and descending rami, and different angulations of the sylvian fissure. HPT: horizontal portion of the planum temporale. X marks the point at which the PT bends in diagram C, and is marked on the other diagrams to illustrate a plausible estimated corresponding point. See text for additional details.

stretching the right arm of the 'Y' (i.e. the ascending ramus) so that it is longer than the descending ramus.

In both the H&V-type case and the variation of that case just described, the vertical wall of tissue at the end of HPT is the posterior wall that is shared in common by the ascending and descending rami. However, this is not always the case. The surface of the HPT, which is roughly flat in the H&V-type PTs, may also be bent (Fig. 1C) or unbent, but wholly tilted (Fig. 1D). In such cases, the nearly vertical tissue rising at the end of the apparent HPT (which may itself sometimes disappear completely if the bend is very close to Heschl's gyrus marking the anterior border of the PT, as in the illustration in Fig. 1D) is not homologous to the posterior wall of the ascending and descending rami. Rather, it is homologous to tissue which would, in the H&V-type PT, constitute the posterior region of HPT. This is illustrated in Figure 1 by shading behind the 'posterior wall' (the name is misleading in case 1D) in each of these cases.

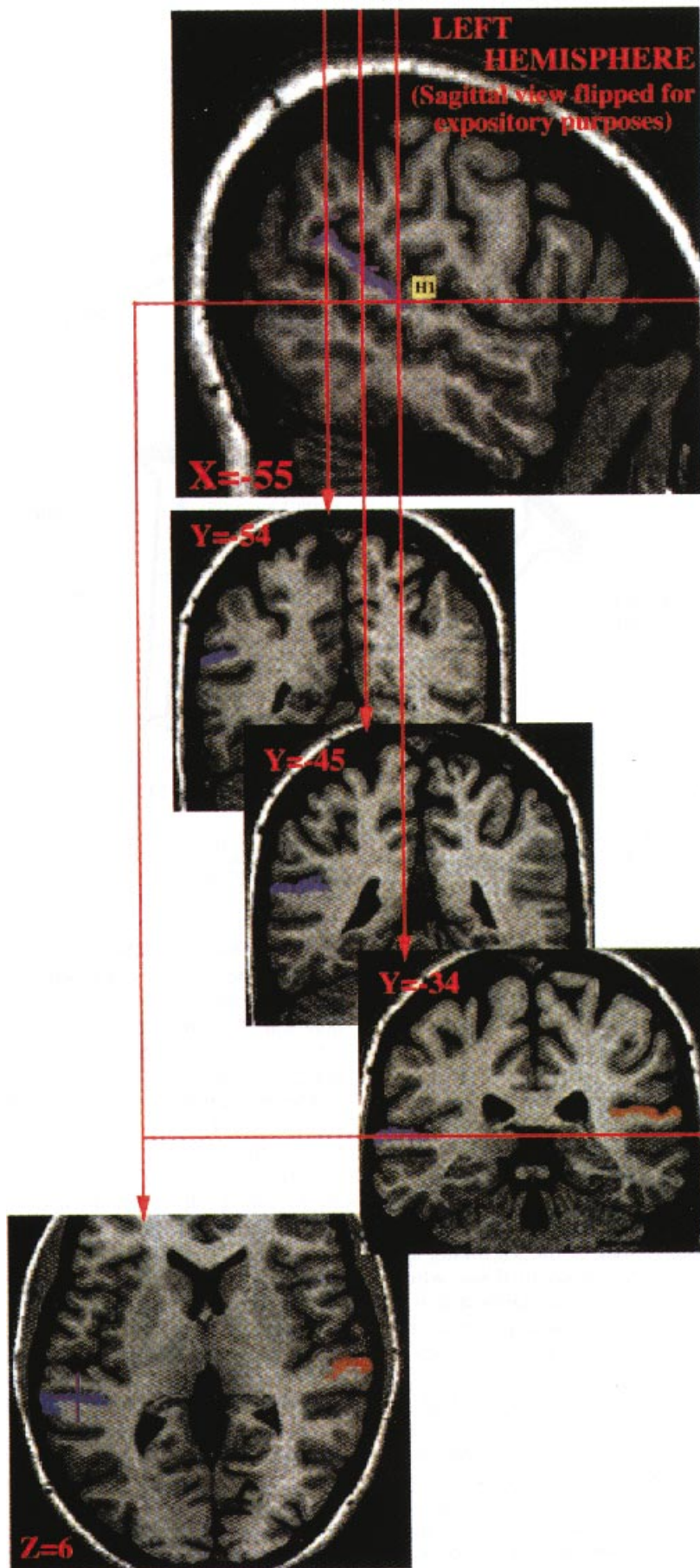
The cartoons in Figure 1 oversimplify the variation of the PT for the sake of ease of exposition. There is another important source of morphological variation which is only hinted at in Figure 1, which is that the ascending and descending rami may themselves vary considerably (and independently) in length. In some cases there may be no apparent rami at all. As one can infer from consideration of Figure 1, it cannot always be possible to

decide by looking only at sagittal sections of an MRI scan whether one is looking at a bent PT with small or nonexistent ascending and descending rami (a variation of Fig. 1C), or a non-bent PT with a small descending ramus (a variation of Fig. 1A or C), since the two cases may appear to be identical on sagittal sections.

The problem is illustrated with MRI data in Figures 3 and 4, which present illustrative sections from two brains examined for this study.

In Figure 3, there is both a strong curvature in the surface of the PT, and a sulcus close behind H1 which appears to be the descending ramus. However, coronal slices through that wall show that the labeled tissue on the three most posterior coronal cuts is continuous with and on the same plane as the labeled tissue on the most anterior coronal cut, which is part of the PT by anyone's criteria (the most anterior labeled region appears on the sagittal cut as if it might be a second Heschl's gyrus, but the coronal and horizontal cuts make clear that it is not). This example illustrates why it is necessary to examine the coronal plane – and sometimes the horizontal plane as well – in order to confirm any alleged identification of the descending ramus which has been made by examining only sagittal cuts.

Figure 4 shows an example of a highly curved temporal surface. Once again, the labeled tissue on the three coronal cuts forms a continuous region of tissue which would be arbitrarily



divided if the end of the PT were deemed to be anywhere anterior on that curved surface.

It is important to emphasize that the difficulty in specifying the posterior border is purely operational, rather than definitional. When all of the relevant landmarks are clearly discernible, there are only minor disagreements about the border, such as whether or not one should consider the posterior wall of the descending ramus to be part of the PT. It is only the fact that the relevant anatomical landmarks are not always clearly discernible that introduces uncertainty. Our goal was to find a way to operationalize our criteria so that the borders of the probability map we generated would be well specified.

### Measuring Asymmetry

Most published papers have standardized the asymmetry measures using an asymmetry index defined as:

$$\frac{(\text{right planum measure} - \text{left planum measure})}{[0.5 \times (\text{right planum measure} + \text{left planum measure})]}$$

The use of this index is motivated by the belief that it is relative, rather than absolute, differences in the size of the PT that are of interest. The asymmetry index therefore only compensates for differences in the region of interest, and does not attempt to compensate for differences in overall brain size. The advent of automated means of standardizing brain size and shape into a normatively defined brain space based on a large sampling of normal brains (Collins *et al.*, 1994) makes it possible to compensate for overall hemispheric differences prior to looking at the region of interest, by providing a means of normalizing anatomical regions of interest based on global rather than local neurological landmarks. This ensures that any transformations in the region of interest will reflect differences in global brain size. In the present study, we opted for this approach because of these advantages, and because it has not usually been applied in prior studies of PT morphometry.

### Creating a Probabilistic Map of the PT

The technical ability to transform brain scans with a labeled region of interest allowed us to produce a probabilistic map of the PT which quantitatively represents the between-subjects variability of the spatial boundaries of the PT as we defined it. Because all subjects' MRI scans are transformed into standardized Talairach-Tournoux space (Talairach and Tournoux, 1988), we are able to determine the probability (within our sample) that each individual voxel within that space falls within the region which defines the PT. The probability map that is generated can be co-registered with data from any other brain or average brain which has been transformed into the same space, making it possible to determine the likelihood that any site of functional activation or any lesion falls within the region of the PT, as we have defined it. A similar approach has already been applied to the region containing primary auditory cortex, Heschl's gyrus (Penhune *et al.*, 1996).

## Materials and Methods

### Subjects

The subjects were 50 healthy normal right-handed volunteers: 29 males

and 21 females. The average age was 25.2 (SD 5.2 years). There were no significant sex differences in age [male average: 25.5 (SD 5.2); female average: 24.9 (SD 5.2);  $P > 0.05$ ].

### Procedure

#### Data Acquisition and Manipulation

Scan data were obtained on a Phillips Gyroscan system with a 1.5 T superconducting magnet. One hundred and twenty-eight 1 mm  $T_1$ -weighted images were acquired in the axial plane ( $T_R = 550$  ms,  $T_E = 30$  ms). Each scan was registered in the standardized stereotaxic space defined by Evans *et al.* (Evans *et al.*, 1992), which is based on the average of 305 MRI brain volumes of normal brains, mapped into the same stereotaxic space [as defined by Talairach and Tournoux (Talairach and Tournoux, 1988)] and normalized for intensity using an automatic procedure (Collins *et al.*, 1994).

#### PT Identification

As explained earlier – and illustrated in Figures 1, 3 and 4 – most complications in identifying the PT arise in identifying the posterior border, especially in those cases in which the Sylvian surface is not flat, and/or there is no unambiguous ascending ramus and/or descending ramus. In order to determine if there might be a more principled solution to the problem of defining the posterior border, we studied a large number of H&V-type PTs, because these are the least controversial cases for discerning the relevant borders. In such cases the following three observations were observed to be true without exception:

1. The transition from the anterior to the posterior border of the descending ramus is marked by an unambiguous transition off the plane of tissue being labeled in coronal cuts.
2. Tissue which was labeled as being in the PT extends all the way to the end of the surface being labeled on every single cut in the coronal view.
3. The PT extends very far back along the Sylvian fissure, i.e. the ascending and descending rami are very small compared to the size of the anterior Sylvian surface.

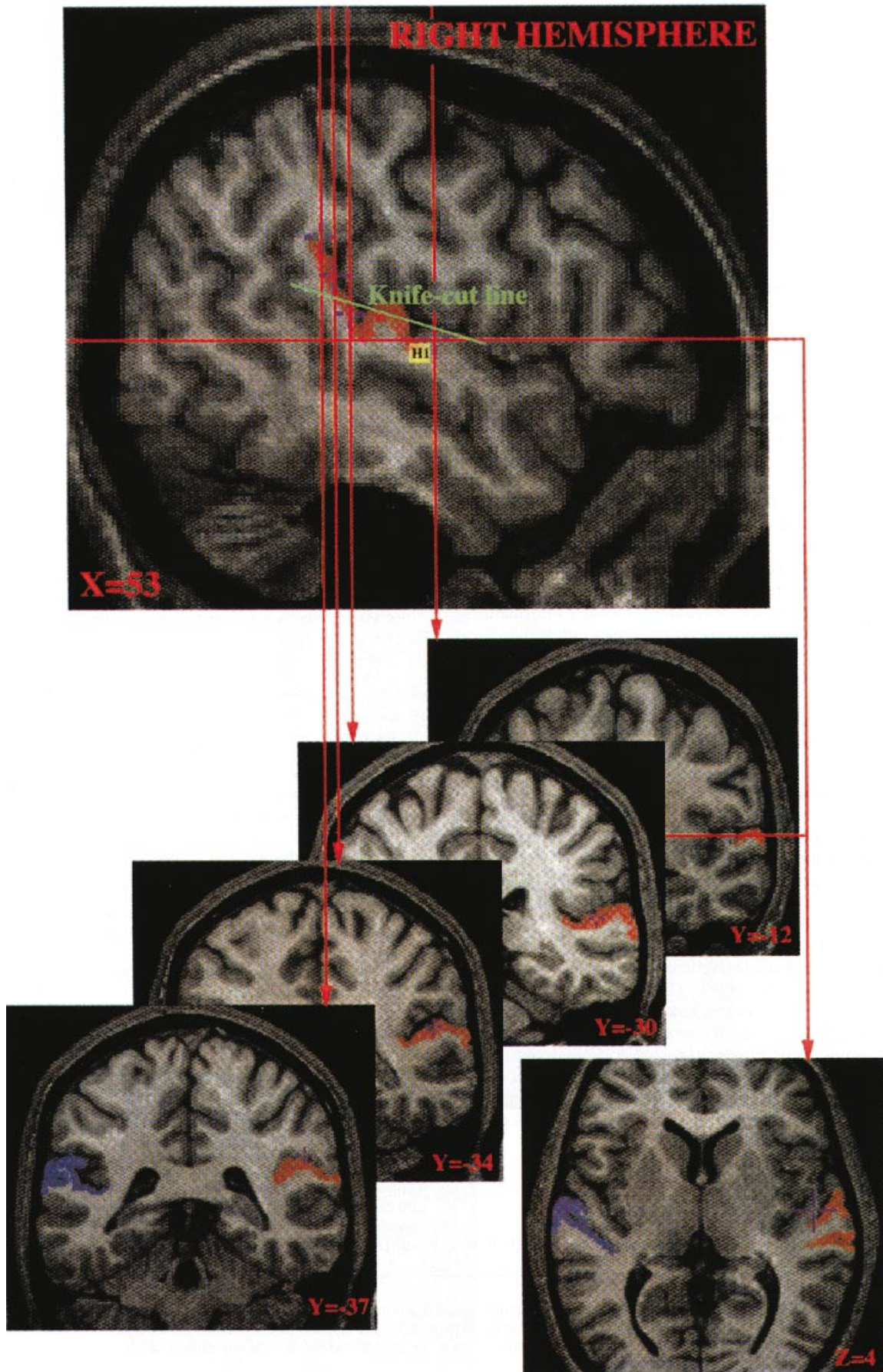
We used this information about the uncontroversial cases to define a set of operational rules for identifying the PT in those controversial cases which lacked a clear ascending or descending ramus. The definition was formulated to try to preserve these three characteristics as well as possible. Based on our study of the H&V-type cases, we defined the posterior border of the PT as either:

1. The point at which a label is clearly no longer on the same plane on coronal cuts as the most anterior label (behind H1), but on the plane above it; or
2. The very end of the Sylvian fissure (in the case where there is no descending ramus at all).

This operational definition was developed solely to accord with the H&V-type cases, since in those cases there is no controversy about how to identify the PT. Its blind application never fails to label the PT in the manner appropriate to such cases, including the anterior (but not the posterior) wall of the descending ramus. Its application in other cases will sometimes label tissue that would be excluded from the PT if one relied on the knife-cut rule.

Note that the first criterion of our operational definition has a general application. In the H&V-type cases, the fact that the transition from the anterior to the posterior border of the descending ramus is marked by an unambiguous transition off the anteriorly labeled surface in coronal cuts is a reflection of the fact that the posterior wall of the descending ramus

**Figure 2.** MRI scans of the least controversial (H-V type) PT. The top panel shows a sagittal slice through the left hemisphere (taken at  $x = -55$ ), with the PT cortical area labeled in blue. The positions of three coronal slices ( $y = -34, -45, -54$ ) are indicated by the three red vertical lines, and each of the three corresponding coronal images is shown below. Note the continuity of the blue-labeled tissue along the Sylvian fissure in the left hemisphere. The bottom image corresponds to a horizontal slice ( $z = 6$ ) showing the commencement of the PT just behind Heschl's sulcus, the posterior border of Heschl's gyrus.



leans forward from the vertical in those cases. However, when there are no ascending or descending rami at all in a PT with a flat HPT, the transition off the temporal surface on coronal cuts occurs at the end point of the Sylvian fissure, which is the point where the descending ramus would be in the uncontroversial H&V-type cases. When there is a fold in HPT which may mimic a descending ramus, the criterion will not label that fold as the descending ramus if the posterior wall in such a fold does not angle forward in such a way as to be marked by a transition between planes on the coronal cuts. In cases in which the surface of HPT has changes in slope which are not marked by any clear rami, the operational criterion will not cut that surface: the entire surface will be labeled as part of the PT.

Although there is no conceptual disagreement about the lateral border of the PT, there is no operational definition of how to label tissue at the border. We defined the lateral border of the PT operationally, using coronal cuts, as that point on the temporal plane which is even (parallel to the temporal plane, which is not always horizontal) with the lowest mesially labeled point on that plane (see Fig. 5). We applied this definition on every coronal cut anterior to the most posterior label on the sagittal cuts. Since the location of this most posterior label is unambiguously dictated by the application of the previous rule for identifying the posterior border, the application of these two operational definitions is absolutely mechanical.

In order to facilitate comparison of our operational definition with previous work which has adopted different criteria for identifying the posterior border of the PT, we also applied the 'knife-cut' method to scans which had been labeled using our rules, by removing all labels which fell above the point defined by a projection parallel to the HPT of the temporal lobe onto the posterior surface (see Fig. 3). To operationalize the application of this rule in cases in which the temporal surface curves mesially, we relied only upon the sagittal slice at  $x \pm 60$  to decide where the cut should be made, slicing off tissue above the identified level of that slice on all other sagittal slices. This is a more conservative application of the method than is usually used, since it will never exclude more tissue than might be excluded if the decision to apply the method could be adjusted at the labeler's discretion anywhere along the  $x$ -axis, but it will sometimes exclude less.

The 50 MRI scans were labeled using DISPLAY software (McDonald, 1996) running on SGI workstations. This software allows simultaneous real-time viewing and voxel-labeling on sagittal, coronal and horizontal planes. Fifteen of the scans (30 hemispheres) were independently labeled by a second person as a reliability measure. That labeler was naive as to the definition of the PT and was trained to blindly apply the operational definition. Both labelers were also blind to side.

Grey/white matter boundaries were thresholded automatically, so that only voxels representing grey matter tissue accepted a label. Estimates for the values of the threshold parameters were derived by filling in a subregion of the region of interest without any thresholds. The values of those labeled voxels were then graphed in a histogram. Discontinuities in the histogram made it possible to visually identify the threshold levels at which the grey/white matter boundary occurred. Both labelers used the same threshold values for determining the grey/white matter border.

Volumetric data were calculated by summing over all labeled voxels. Surface area measurements were automatically calculated, using a method defined previously (McDonald, 1996). DISPLAY allows its user to specify areas which are not to be included in the surface calculation. We excluded both the grey/white matter interfaces and the area of the grey/grey matter borders between labeled and unlabeled voxels, in order to obtain a measure only for the cortical surface.

The software also makes it possible for us to examine the labeled surface by lifting it from the cortex, and rotating it in three dimensions, allowing us to verify by visual inspection that all non-desired tissue is excluded.

**Table 1**

Averages, SDs, 1 and 2 SD cut-offs, and measures of skewness and kurtosis of the asymmetry measures of this sample

	Cut volume	Cut area	Uncut volume	Uncut area
Skew	-0.42	-0.57	-0.02	-0.09
Kurtosis	-0.18	0.09	-0.11	0.48
Average	-0.13	-0.17	-0.05	-0.06
SD	0.41	0.43	0.39	0.39
Ave. $\pm$ 1SD	0.28/-0.55	0.26/-0.60	0.35/-0.44	0.33/-0.45
Ave. $\pm$ 2SD	0.70/-0.96	0.69/-1.04	0.74/-0.83	0.71/-0.83

## Results

### Interhemispheric Asymmetries

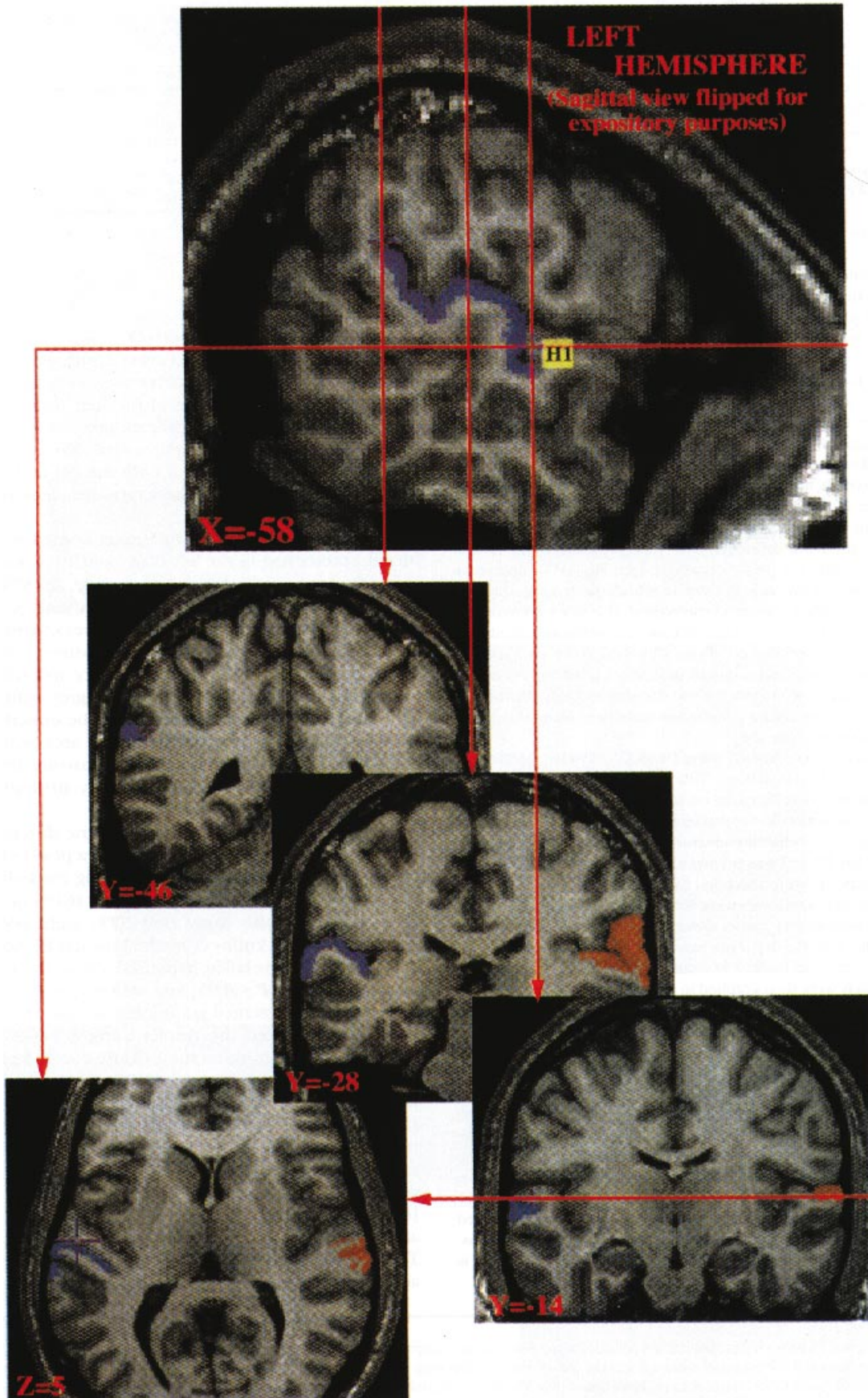
The averages, SDs, 1 and 2 SD cut-offs, and measures of skewness and kurtosis of the asymmetry measures of our sample are presented in Table 1. None of the four distributions of asymmetry scores (area and volume measures of cut and uncut plana) depart significantly from normality. We also examined the distribution characteristics of both the cut and uncut area and volume measures. None of these measures departed significantly from normality.

Twenty-seven (55%) of the brains labeled using the operational criteria had larger left than right PT volumes and areas. After the application of the knife-cut rule, 28 (57%) of the brains had larger left than right PT volumes, and 32 (65%) of the brains had larger left than right PT areas. Area measures are more open to error than volumetric measures, since the method used does not allow us to measure surface area which lies within a convolution. Since the depth of the grey matter is relatively constant, the volume measures should be directly proportional to the real surface area, including the area which lies buried within cerebral convolutions. The departure from this direct proportionality may probably be largely attributed to errors in measuring the area.

There were no significant hemispheric differences in either PT volume [ $t(49) = 0.38$ ;  $P > 0.05$ ] or area [ $t(49) = 0.20$ ;  $P > 0.05$ ] within the scans labeled before applying the knife-cut method. The knife-cut rule was applicable to 60 (61%) of the 98 labeled hemispheres in the study (left 57%; right 65%). After the application of the knife-cut method the left PT was significantly larger (under a one-tailed hypothesis) than the right in surface area [ $t(49) = 2.5$ ;  $P < 0.05$ ] and volume [ $t(49) = 2.0$ ;  $P < 0.05$ ]. These data are presented graphically in Figure 6.

We also analyzed the results using a  $2 \times 2 \times 2 \times 2$  [side (left/right)  $\times$  labeling method (knife-cut/no-knife-cut)  $\times$  size measure (volume/area)  $\times$  sex] ANOVA. Only the main effects of labeling method [ $F(1,49) = 59.41$ ;  $P < 0.0001$ ] and size measure [ $F(1,49) = 554.75$ ;  $P < 0.0001$ ] were significant, reflecting, respectively, the fact that the application of the knife-cut method significantly reduces the size of the PT, and the fact that areas are smaller than volumes. There was no main effect of side [ $F(1,49) = 2.13$ ;  $P > 0.05$ ] or sex [ $F(1,48) = 0.16$ ;  $P > 0.05$ ], nor any significant two-way interaction effects involving side or sex. There was a significant interaction between labeling method and size measure [ $F(1,49) = 54.89$ ;  $P < 0.0001$ ], reflecting the

**Figure 3.** MRI scans of a PT with a marked vertical component. The top image shows a sagittal section taken through the right hemisphere ( $x = 53$ ), with the PT tissue labeled in red, and with the positions of the four coronal slices indicated by red vertical lines. The most anterior coronal cut ( $y = -12$ ) is taken through the body of Heschl's gyrus, which is visible as the more medial gyrus in the coronal section shown below. Heschl's gyrus is also visible in the horizontal view ( $z = 4$ ), which illustrates the anterior border of the PT in this brain. The other three coronal sections ( $y = -30, -34, -37$ ) illustrate the complete continuity of the labeled PT tissue along the superior temporal surface.



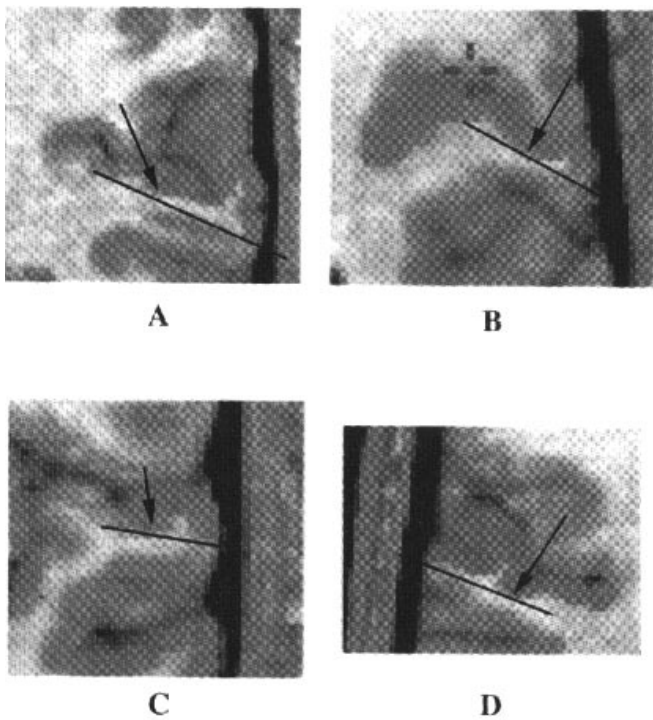


**Figure 5.** Four illustrations, taken from coronal sections, showing how the lateral border of the PT was labeled in this study. The lateral border was defined as that point on the temporal surface which is even, parallel to the temporal plane, with the lowest mesially labeled point on that plane. The lowest point is marked with an arrow, and the black line is parallel to the end of the temporal plane. [Note that sometimes, as in (B), this line will not be parallel to the entire surface since that surface may bend at the end.] The lowest point is easily labeled using other criteria (see text). Such a rule is necessary for deciding where to stop labeling when the coronal cuts slice through nearly vertical sections of the PT, in which case the PT appears to ‘mushroom’ on coronal cuts, as in example (A).

fact that the application of the knife-cut method reduces the disparity between volume and area. There were no significant three- or four-way interaction effects.

The volumetric and area measure data are summarized in Figure 6, which also makes clear that there is considerably more variance in the size of the right PT than in the size of the left PT. To try to understand in more detail how the area and volume differences arose, we examined the points which defined the bounding box of the PTs (i.e. the smallest rectangular box which could contain all the labeled voxels of the PT) defined using each labeling method, and examined the differences in the extent of that box along each dimension. Within the cut and uncut PTs, only the length of the bounding box along the *y* (anterior/posterior) dimension differed significantly between sides [cut:  $t(48) = -5.19$ ;  $P < 0.001$ ; uncut:  $t(43) = -2.89$ ;  $P < 0.01$ ]. These differences are illustrated in Figure 7.

It is clear from inspection of Figure 7 that the application of the knife-cut rule has a greater effect on the right side than the left. In order to quantify the extent of this difference, we calculated the slope across the diagonal of the bounding box of each PT (i.e. the slope from the most inferior, posterior, lateral

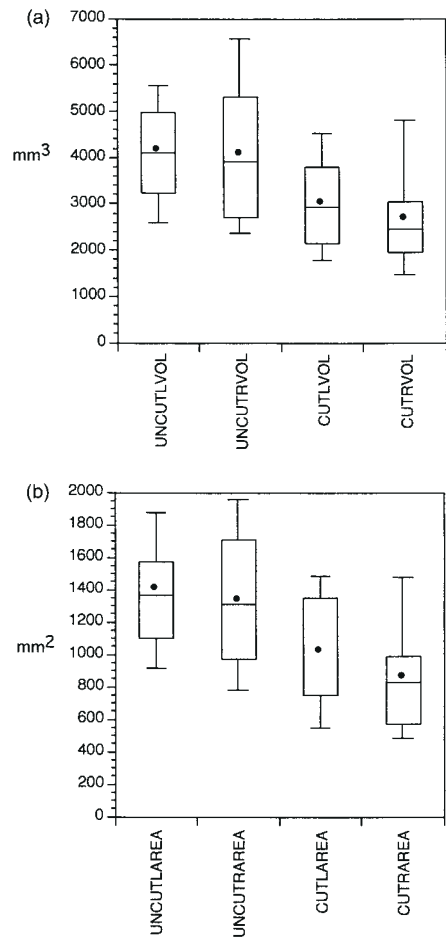


**Figure 6.** Summary of PT volumes and areas by hemisphere and label-type (i.e. with and without the application of the knife-cut rule). Black circles mark the population mean. The vertical boundaries of the box mark the 25th and 75th percentiles. The horizontal line within the box marks the 50th percentile. The bars mark the 10th and 90th percentiles. Note that the right hemispheres exhibit considerably more variation than the left hemispheres, especially in the uncut condition.

point to the most superior, anterior and mesial point within each bounding box). The right slopes were significantly steeper than the left side in the uncut condition [ $t(48) = 2.692$ ;  $P < 0.05$ ] but not in the cut condition [ $t(43) = 0.964$ ;  $P > 0.05$ ].

There were no significant interactions of slope differences by sex in either the cut or uncut PTs.

### Probabilistic Mapping

Sagittal slices (4 mm) through the PT probability map are reproduced in Figure 8. Horizontal slices are reproduced in Figure 9. No voxel appeared in more than 65% of the labeled PTs. As in Figure 7, it is clear from inspection of the probability maps that the variability on the right side is greater than on the left. It is also apparent that the border of the probabilistic posterior PT on the right side flares up at a greater angle and to a greater height than the right side than the left, especially at the lateral

**Figure 4.** MRI scans of a PT with a highly curved segment. The top image shows a sagittal section through the left hemisphere ( $x = -58$ ) illustrating the undulating temporal surface observed in this brain, with the PT tissue labeled in blue. The three coronal sections shown below indicate that the blue-labeled tissue forms a continuous band from  $y = -14$  to  $y = -46$ , which would be arbitrarily divided if the end of the PT were deemed to be anywhere anterior. The anterior boundary of the PT is best seen in the horizontal section ( $z = 5$ ), which shows the clear demarcation afforded by Heschl’s sulcus.

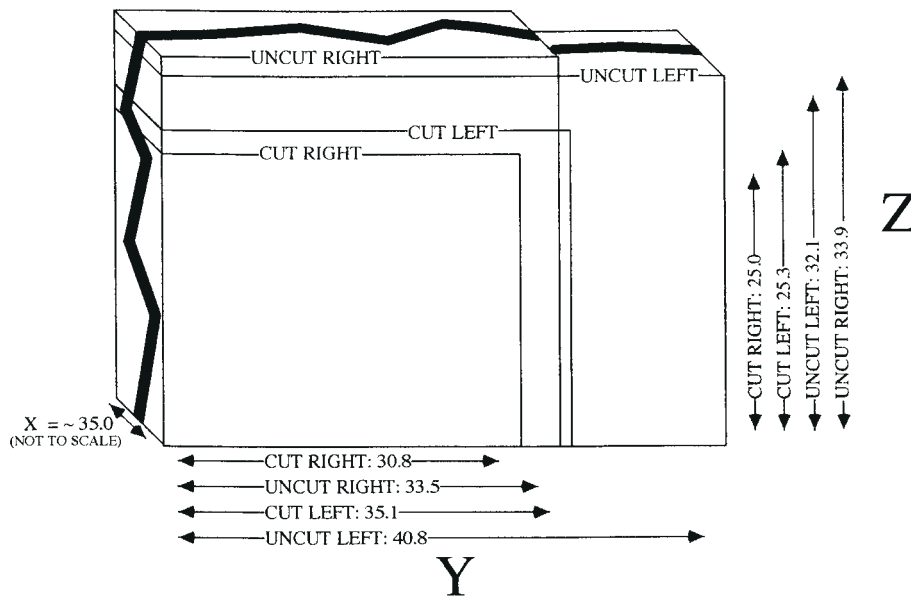


**Figure 7.** Bounding box data. Here the bounding boxes for the four conditions of interest (hemisphere  $\times$  label-type) have been superimposed on top of each other. As the knife-cut rule does not affect the  $x$ -axis and there is little variation between hemispheres on that axis, it has been compressed for simplicity of presentation. All measures are in millimeters. Only the length of the bounding box along the  $y$  dimension differs significantly between sides. This figure shows that hemispheric differences in the PT are due in large part to the fact that the horizontal component of the uncut PT is larger in the left than on the right.

edge, suggesting that the right hemispheres contain higher and more angled PTs than the left does.

The PT picked out by the application of the knife-cut method is a subset of the area picked out by the operational criteria we used. The probability maps generated using the latter criteria may therefore be used to localize activation to the PT as defined by the former. As illustrated in Figures 7 and 8, the difference is that a region of the probability maps for each hemisphere needs to be ignored (i.e. assigned a probability value of 0) if one is using the definition proposed by the knife-cut method, since that method excludes tissue in that region. On the right, the average region falling outside the PT as defined by the knife-cut rule covers the three-dimensional L-shaped area comprising the posterior 2.7 mm and the superior 8.9 mm of the region with non-zero probability shown in Figure 8. On the left, the average region which falls outside the PT defined by the knife-cut method covers the posterior 5.7 mm and the superior 7.8 mm of the non-zero probability region in Figure 8.

### Reliability

One of the 15 scans randomly selected to be double-coded for reliability was found to be too ambiguous to code, because the posterior wall at the end of the HPT was almost perfectly vertical, revealing a weakness in our operational rule for identifying the posterior border: a judgment call is required to decide whether or not labeled tissue is on a new plane when the coronal slice is through tissue that is nearly vertical. Because of our desire to label tissue in an operationally certain manner, this PT was removed from further consideration.

The surface areas were significantly correlated ( $P < 0.01$ ) at 0.86 (left areas 0.71; right areas 0.95). The volumetric measures were significantly correlated ( $P < 0.01$ ) at 0.86 (left volumes 0.73; right volumes 0.91). The two labelers agreed on the direction of volumetric difference (i.e. on the sign of the L - R volume differences) in 11 out of the 14 doubly coded cases. All three disagreements were 'borderline' cases in which the L - R differences were very small (see Fig. 10). The overall level of

reliability attained by the application of our operational rules alone was comparable to that in other studies using similar MRI-based morphometric methods [i.e. Steinmetz *et al.* (Steinmetz *et al.*, 1995) report three inter-rater reliability measures ranging from 0.82 to 0.87; Jancke *et al.* (Jancke *et al.*, 1993) report asymmetry correlation coefficients, using a different measure, ranging between 0.80 for the vertical portion and 0.91 for the horizontal portion of the PT]. Previous studies have not broken down inter-rater correlation coefficients by hemisphere.

### Discussion

We found no evidence of significant volume or area asymmetries in the PT between hemispheres except when the 'knife-cut' rule was used, in which case we did find a significant difference in both area and volume. Since more tissue is cut from the right than the left side when the knife-cut rule is applied, the right PT must tend to slope more sharply from the surface of the Sylvian fissure than the left PT. The difference is visible by comparing average PT bounding boxes on each side (Fig. 7) and in the probability maps made from averaging all labeled PTs (Figs 8 and 9).

Since our definition differs in just over 60% of cases seen in this study from the most widely used definition of the PT using the knife-cut method, the question of validity must be addressed. Is one definition valid and another invalid? This question arises because of a simple fact: the PT has no consistent, definite natural boundaries, and thus has the necessarily shaky ontological status of all human constructs, including many anatomical and biological structures.

The validity of a construct ultimately depends on convergent evidence from independent data sources that are accepted to reflect the same hypothesized entity that the construct does. The requirement of independence means that we cannot simply appeal to consistency with previous studies which relied upon one definition as evidence against a different definition. Such dependent consistency speaks to the reliability of the definition,

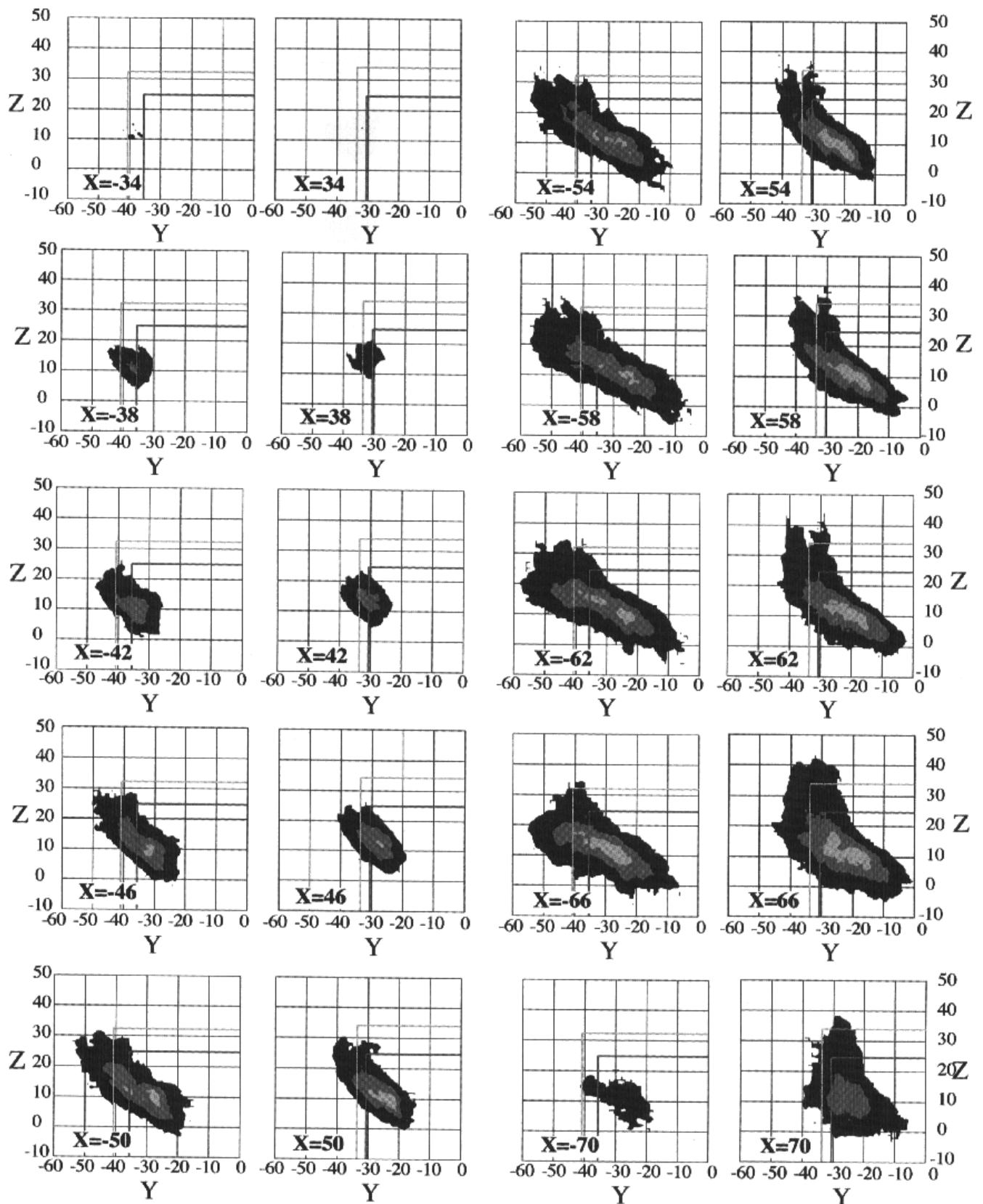


**Figure 8.** Sagittal cuts every 4 mm through the probability map in Talairach space which was obtained by averaging together all PTs labeled using our criteria. Black areas appeared in 5–25% of labeled PTs; dark grey areas appeared in 26–45% of PTs; and light grey areas appeared in 46–65% of PTs. The extended HPT of the left PT and the extended VPT of the lateral right PT are clearly visible. The average bounding boxes for the uncut (outer, lighter box) and cut (inner, darker box) PTs are overlaid on each cut to allow for a rough comparison of the differences in the two measures. See also Figure 9.

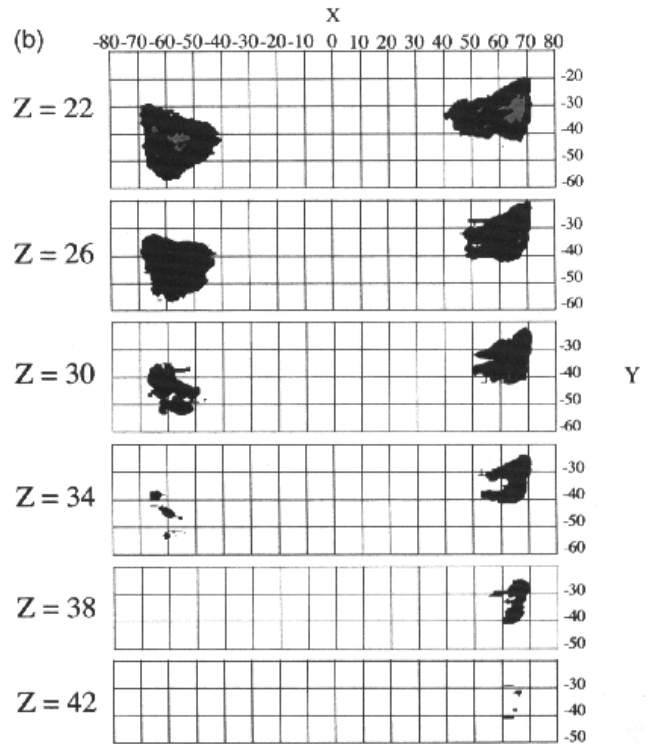
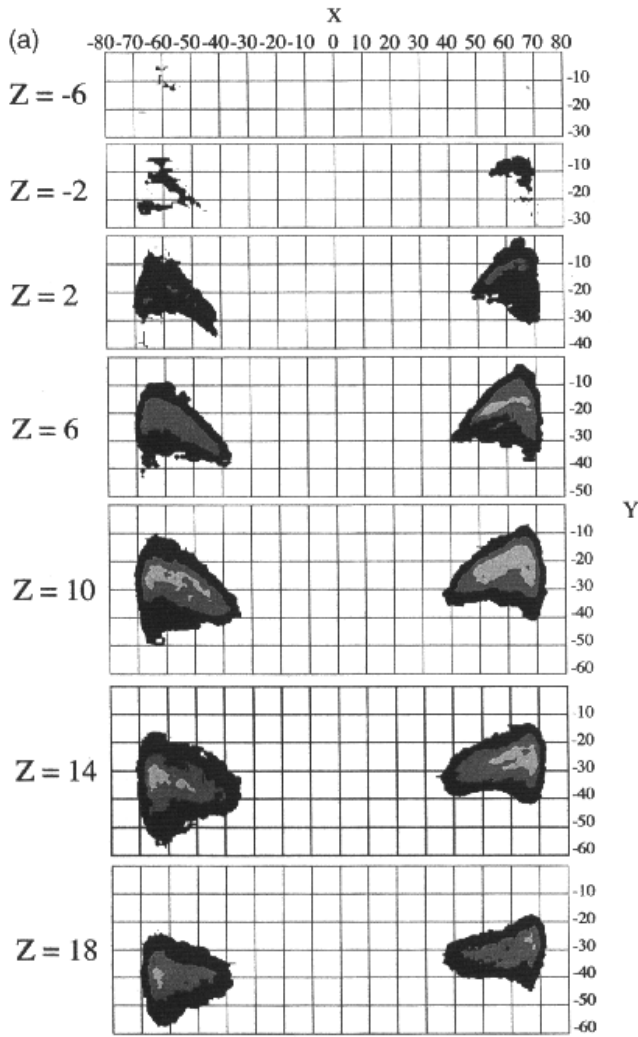


**Figure 9.** Horizontal cuts every 4 mm through the probability map in Talairach space which was obtained by averaging together all PTs labeled using our criteria. Black areas appeared in 5–25% of labeled PTs; dark grey areas appeared in 26–45% of PTs; and light grey areas appeared in 46–65% of PTs. The larger HPT of the left PT and the larger VPT of the lateral right PT are clearly visible.

but not to its validity. The definition we have proposed is consistent with independent bodies of knowledge with which the knife-cut method is inconsistent. First, it is consistent with the larger body of neuroanatomical definitions in ways which the knife-cut method is not. Second, it achieves a better consistency of form between the unambiguous and ambiguous forms. Third, it is more consistent (but not wholly consistent) with the known cytoarchitectonics of the region under consideration.

The definition we offer is consistent with the larger body of neuroanatomical definitions insofar as it defines the PT to be a structure which shares qualities with other cortical regions: it has a consistent general shape (an undulating triangle) whose variants can be easily understood in terms of differences in rotation and stretching, and which never disappears altogether. The knife-cut method, in contrast, defines a structure which varies widely in shape, with ~40% of the structures (based on the number of PTs to which the knife-cut method was applicable in this study) having a triangular shape, and the remainder varying from roughly triangular to a mere speck of tissue, and sometimes disappearing altogether. Although there is wide variation in the gyrification pattern of the human brain, we believe that the most parsimonious explanations for that variation will account for it in terms of continuous quantitative variation along well-defined

dimensions, rather than explanations which postulate qualitative neuroanatomical discontinuities.

The second consistency is a related one: the knife-cut method defines PT structures which vary discontinuously from

the most common, easily defined and uncontroversial variant, the H&V-type variant, which accounted for 40% of the structures in this study. In contrast, the definition we proposed was grounded in the assumption that the atypical variants must share defining characteristics with the H&V-type PTs, and was formulated specifically to preserve three well-defined characteristics of those PTs, as outlined in the Materials and Methods section above. Those three characteristics are not preserved by the knife-cut method. Our ability to independently rotate and examine labeled tissue in three dimensions was a primary source of information in formulating the definition. It was also used to assess its *post-hoc* face validity: tissue labeled using the operational definition we used is morphologically similar to labeled tissue from the unambiguous PTs, inasmuch as it consists of a rough triangular shape, which has the additional characteristic of being folded or rippled.

Finally, the operational definition we used is more consistent with the known cytoarchitectonics of the region under consideration than the definition used by the knife-cut method. Cytoarchitectonic analyses (Galaburda *et al.*, 1978; Witelson *et al.*, 1995) have shown that that area TA1 [which Galaburda *et al.* (Galaburda *et al.*, 1978) call area Tpt; see Witelson *et al.* (Witelson *et al.*, 1995) for a detailed cytoarchitectonic description of the area, which cannot be identified by gross anatomy alone], located in the posteriormost region of HPT, is also found

## 2 LABELERS; L - R VOLUMES

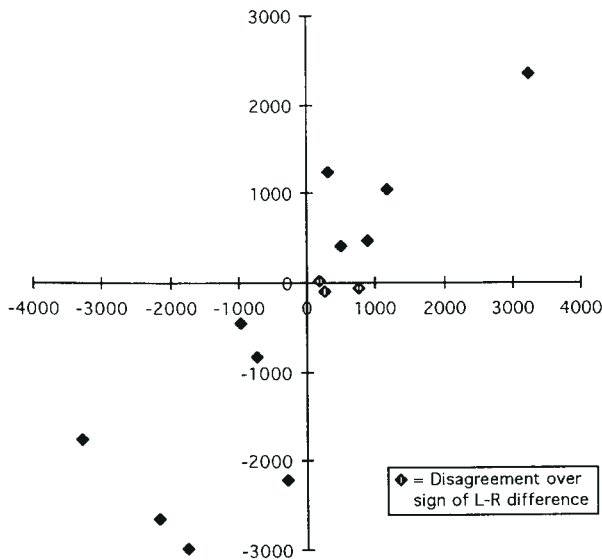


**Figure 10.** Reliability measures for two independent labelers. The volumetric measures were significantly correlated ( $P < 0.01$ ) at 0.86 (left volumes 0.73; right volumes: 0.91).

in VPT. Galaburda *et al.* (Galaburda *et al.*, 1978) noted there can be sometimes be more TA1 in the superior temporal gyrus outside of HPT than there is in HPT itself. Witelson *et al.* (Witelson *et al.*, 1995) reported that in all three (from a sample of 18) of the hemispheres they examined which had no HPT at all, TA1 tissue was found in VPT cortex. This finding lends further support to a definition of the PT, such as our operational definition, which defines the tissue in superior VPT as homologous to the posterior region of HPT in the uncontroversial (H&V type) cases of the PT.

A neuroanatomical criterion for identifying the PT which captures this cytoarchitectonic similarity between tissue in the posterior region of HPT and tissue in the superior region of VPT is preferable to one which does not. However no gross anatomical definition of the PT region perfectly captures the documented cytoarchitectonic variation in this region. It has been shown that TA1 can in some cases actually extend beyond the VPT, onto the parietal convexity above (Galaburda *et al.*, 1978) [see also Binder *et al.* (Binder *et al.*, 1996)]. The cytoarchitectonic variability thus is not constrained by even the most unambiguous gross neuroanatomical boundary.

Galaburda *et al.*'s (Galaburda *et al.*, 1978) finding of TA1 tissue extending into the parietal lobe adds a possible complication to any functional interpretation of the PT's role in studies in which the PT is identified by gross neuroanatomy. The issue of functional localization in this region is further complicated by the fact that functional boundaries need not necessarily closely correspond to cytoarchitectonic boundaries. Further study is necessary to determine the probability with which the functional regions normally inside the region in our probability map can also fall outside it. If the variation is rare, then it can be handled in the same time-honored manner for handling variation that the probability map uses: by averaging.

The operational definition adopted in this study has at least two other clear limitations, along with its failure to conform to known cytoarchitectonic variation. First of all, it fails to account

for all cases, since it cannot be unambiguously applied if the posterior wall behind HPT rises at an angle that is very close to vertical. Secondly, its reliance on the angle of a fissure as a sign for the posterior border is justified *a priori* only by the clear validity of that sign in unambiguous cases. Although the sign had good face validity (i.e. accorded well with *post-hoc* human judgment of its plausibility) when applied to the ambiguous cases in our study, it is impossible to guarantee from our judgment of its utility with this sample that it will have universal applicability in all other cases.

The disparity between the asymmetry results obtained using our operational definition of the PT, and the results obtained by the application of the 'knife-cut' rule are in accord with a large body of previous work which has suggested that PT asymmetry reported in the literature reflects a difference in the morphology rather than the size of the PT. Over a century ago Cunningham (Cunningham, 1892) [as cited in Binder *et al.* (Binder *et al.*, 1996)] stated that the right planum was tilted forward more than the left. The precise topological difference in the point at which the posterior PT curves up was first observed in the composite tracings of brain slides by Rubens *et al.* (Rubens *et al.*, 1976) who concluded that 'in many brains the planum temporale is longer on the left because the horizontal portion, but not necessarily the entire length of the lateral fissure, is longer on the left' (p. 623). Many other studies have shown that the right PT shows a greater likelihood of bending than the left PT (Ono *et al.*, 1991; Steinmetz and Galaburda, 1991; Steinmetz *et al.*, 1990; Witelson and Kigar, 1992). Steinmetz *et al.* (Steinmetz *et al.*, 1990) reported a dissociation in ten cadaver brains between the asymmetry index of HPT (which showed a significantly larger left than right surface area) and that of 'the surface of cortex buried in the caudal segments of the Sylvian fissure posterior to the planum' (i.e. VPT), which was on average significantly larger on the right than the left. Loftus *et al.* (Loftus *et al.*, 1993) suggested as a possible interpretation for their results studying contour models of 10 brains that 'the asymmetry of the PT is a side-effect of the more anterior upswing of the Sylvian fissure on the right' (p. 354). Binder *et al.* (Binder *et al.*, 1996), upon finding that the sum of the horizontal and non-horizontal PT areas did not differ between hemispheres, concluded that 'it is the shape rather than the size of the posterior Sylvian fissure that is asymmetric' (p. 1245).

The relation between the morphological asymmetry in the PT and functional asymmetries, especially of language, is still unclear, particularly since language-related functional asymmetries clearly occur with a much higher frequency than PT asymmetries do. Moreover, although some studies have uncovered such relationships [e.g. Foundas *et al.* (Foundas *et al.*, 1994)], others have not [e.g. Jancke *et al.* (Jancke *et al.*, 1993)]. It seems to us unlikely that a relation between a complex linguistic function and a structural asymmetry can be simply attributed to differences in the amount of cortical tissue in the PT on each side of the brain. The implicit assumption behind this view is that a greater amount of tissue is required on the left because auditory language processing is inherently more complex than other types of auditory processing. An alternative point of view is that auditory language processes may require different types of processing than nonlinguistic processes, which might be reflected in different morphology, rather than greater or lesser amounts of tissue. For example, processing of phonetic information may require analysis of rapidly changing broad-band acoustic energy (Tallal *et al.*, 1993; Belin *et al.*, 1998), which

might be related to differential degree of myelination of auditory cortical areas (Penhune *et al.*, 1996).

In this context, it is of interest to note that some studies that have succeeded in demonstrating structure–function correlations have measured arteriographic asymmetries (Hochberg and Le May, 1975; Ratcliff *et al.*, 1980). These findings suggest that morphological differences in the region may be directly relevant functionally, since arteriographic measures are only sensitive to morphology, not to volume or area. As a further possibility, Binder *et al.* (Binder *et al.*, 1996) have suggested that the morphological asymmetries in the PT may be due to a larger frontal and peri-rolandic mass on the left, which may push on the PT, tilting it back and pushing the point of deflection of the Sylvian fissure posteriorly, and to a larger posterior parietal lobe on the right, which might push on the PT from behind in such a way as to tilt it forward and move the deflection point anteriorly. This suggestion, that functional differences in the PT may reflect anatomical structural differences in other regions which impinge on the PT, suggests a promising avenue for future work aimed at clarifying the structure–function relationship in this area.

We propose that the technique of probability mapping obtained by averaging together labeled tissue, as used in the present study, may provide a useful means for future study of the relationship between cerebral morphology and function. If the relationship between brain structure and function depends on subtle morphological features, rather than frank size differences, then probability mapping could help to uncover such relationships. For example, comparisons of PT probability maps could be carried out to examine differences among subjects with known left- or right-hemisphere mediated language functions. The same approach may also ultimately prove useful in examining putative structural abnormalities of the PT region, such as have been described for schizophrenia (Petty *et al.*, 1995; Falkai *et al.*, 1995), or for dyslexia (Leonard *et al.*, 1993; Rumsey *et al.*, 1997).

## Notes

We thank Raquel Dorsaint-Pierre and Greg Ward for their assistance. Supported by funds from the Medical Research Council of Canada (MT11541), the McDonnell–Pew Program in Cognitive Neuroscience, and the International Consortium for Brain Mapping, an initiative of the Human Brain Project.

Address correspondence to C.F. Westbury, Department of Psychology, P220 Biological Sciences Building, University of Alberta, Edmonton, Alberta, Canada T6G 2E5. Email: [chrismw@ualberta.ca](mailto:chrismw@ualberta.ca).

## References

- Aboitiz F, Scheibel AB, Zaidel E (1992) Morphometry of the sylvian fissure and the corpus callosum, with emphasis on sex differences. *Brain* 115:1521–1541.
- Barta PE, Petty RG, McGilchrist I, Lewis RW, Jerram M, Casanova MF, Powers RE, Brill LB, Pearlson GD (1995) Asymmetry of the planum temporale: methodological considerations and clinical associations. *Psychiat Res Neuroimaging* 61:137–150.
- Belin P, Zilbovicius M, Crozier S, Thivard L, Fontaine A, Masure M-C, Samson Y (1998) Lateralization of speech and auditory temporal processing. *J Cogn Neurosci* 10:536–540.
- Binder JR, Frost JA, Hammeke TA, Rao SM, Cox RW (1996) Function of the left planum temporale in auditory and linguistic processing. *Brain* 119:1239–1247.
- Bossy J, Godlweski G, Maurel J-C (1976) Etude de l'asymétrie droite–gauche du planum temporale chez le fœtus. *Bull Assoc Anat* 60:253–258.
- Chi JG, Dooling EC, Gilles FH (1977) Left–right asymmetries of the temporal speech areas of the human fetus. *Arch Neurology* 34:346–348.
- Crichton-Browne J (1880). On the weight of the brain and its component parts in the insane. *Brain* 2:42–67.
- Cunningham DJ (1892). Contribution to the surface anatomy of the cerebral hemispheres. Dublin: Royal Irish Academy.
- Falkai B, Bogerts B, Schneider T, Greve B, Pfeiffer U, Pilz K *et al.* (1995) Disturbed planum temporal asymmetry in schizophrenia: a quantitative post-mortem study. *Schizophr Res* 14:161–176.
- Falzi G, Perrone P, Vignola LA (1982) Right–left asymmetry in the anterior speech region. *Arch Neurol* 39:239–240.
- Foundas AL, Leonard CM, Gilmore R, Fennell E, Heilman KM (1994) Planum temporale asymmetry and language dominance. *Neuropsychologia* 32:1225–1231.
- Galaburda AM, LeMay M, Kemper TL, Geschwind N (1978a) Right–left asymmetries in the brain: structural differences between the hemispheres may underlie cerebral dominance. *Science* 199:852–856.
- Galaburda AM, Sanides F, Geschwind N (1978b) Human brain: cytoarchitectonic left–right asymmetries in the temporal speech region. *Arch Neurol* 35:812–817.
- Galaburda AM, Corsiglia J, Rosen G, Sherman GF (1987) Planum temporale asymmetry, reappraisal since Geschwind and Levitsky. *Neuropsychologia* 25:853–868.
- Geschwind N, Levitsky W (1968) Human brain: left–right asymmetries in temporal speech region. *Science* 161:186–187.
- Habib M, Robicon F, LÉvrier O, Khalil R, Salamon G (1995) Diverging asymmetries of temporo-parietal cortical areas: a reappraisal of the Geschwind/Galaburda theory. *Brain Lang* 48:238–258.
- Hochberg FH, LeMay M (1975) Arteriographic correlates of handedness. *Neurology* 25:218–22.
- Ide A, Rodriguez E, Zaidel E, Aboitiz F (1996) Bifurcation patterns in the human sylvian fissure: hemispheric and sex differences. *Cereb Cortex* 6:717–725.
- Jäncke L, Steinmetz H (1993) Auditory lateralization and planum temporale asymmetry. *NeuroReport* 5:169–172.
- Jäncke L, Schlaug G, Huang Y, Steinmetz H (1993) Asymmetry of the planum parietale. *NeuroReport* 5:1161–1163.
- Karbe H, Würker M, Herholz K, Ghaemi M, Pietrzyk U, Kessler J, Wolf-Dieter H (1995) Planum temporale and Brodmann's area 22: magnetic resonance imaging and functional positron emission tomography demonstrate functional left–right asymmetry. *Arch Neurol* 52:869–874.
- Kopp N, Michel F, Carrier H, Biron A, DuVillard P (1977) Etude de certaines asymétries hémisphériques du cerveau humain. *J Neurol Sci* 34:349–363.
- Kulynych JJ, Vldar K, Jones DW, Weinberger DR (1993) Three-dimensional surface rendering in MRI morphometry: a study of the planum temporale. *J Comput-Assist Tomogr* 17:529–535.
- Kulynych JJ, Vldar K, Jones DW, Weinberger DR (1994) Gender differences in the normal lateralization of the supratemporal cortex: MRI surface-rendering morphometry of Heschl's gyrus and the planum temporale. *Cereb Cortex* 4:107–118.
- Leonard CM, Voeller KKS, Lombardino LJ, Morris MK, Hynd GW, Alexander AW, *et al.* (1993) Anomalous cerebral structure in dyslexia revealed with MRI. *Arch Neurol* 50:461–469.
- Loftus WC, Tramo MJ, Thomas CE, Green RL, Nordgren RA, Gazzaniga MS (1993) Three-dimensional quantitative analysis of hemispheric asymmetry in the human superior temporal region. *Cereb Cortex* 3:348–355.
- Loftus WC, Tramo MJ, Gazzaniga MS (1995) Cortical surface modeling reveals gross morphometric correlates of individual differences. *Hum Brain Map* 3:257–270.
- McGlone J (1980) Sex differences in human brain symmetry: a critical survey. *Behav Brain Sci* 3:215–263.
- Musilino A, Dellatolas G (1991) Asymétries du cortex chez l'homme évaluées *in vivo* par agiographie stéréotaxique–stéréoscopique: corrélations anatomo-fonctionnelles. *Rev Neurol* 147:35–45.
- Ono M, Kubik S, Abernathy CD (1991) Atlas of the cerebral sulci. New York: Thieme.
- Penhune VB, Zatorre RJ, MacDonald JD, Evans AC (1996) Inter-hemispheric anatomical differences in human primary auditory cortex: probabilistic mapping and volume measurement from magnetic resonance scans. *Cereb Cortex* 6:661–672.
- Petty RG, Barta PE, Pearlson GD, McGilchrist IK, Lewis RW, Tein AY (1995) Reversal of asymmetry of planum temporal in schizophrenia. *Am J Psychiat* 152:715–721.

- Pfeifer RA (1936) Pathologie der Hörstrahlung und der corticalen Hörsphäre. In: Handbuch der Neurologie, Vol. 6 (Bumke P, Foerster O, eds), pp. 533–636. Berlin: Springer-Verlag.
- Pieniadz JM, Naeser MA (1984) Computed tomographic scan cerebral asymmetries and morphologic structures: correlations of the same cases post mortem. *Arch Neurol* 41:403–409.
- Ratcliff G, Dila C, Taylor L, Milner B (1980) The morphological asymmetry of the hemispheres and cerebral dominance for speech: a possible relationship. *Brain Lang* 11:87–98.
- Rademacher J, Caviness VS, Steinmetz H, Galaburda AM (1993) Topographical variation of the human primary cortices: complications for neuroimaging, brain mapping, and neurobiology. *Cereb Cortex* 3:313–329.
- Rubens AB, Mahowald MW, Hutton T (1976) Asymmetry of the lateral (sylvian) fissures in man. *Neurology* 26:620–624.
- Rumsey JM, Donohue BC, Brady DR, Nace K, Giedd GN, Andreason P (1997) A magnetic resonance imaging study of planum temporale asymmetry in men with developmental dyslexia. *Arch Neurol* 54:1481–1489.
- Steinmetz H, Galaburda AM (1991) Planum temporale asymmetry: in-vivo morphometry affords a new perspective for neurobehavioral research. *Reading Writing* 3:331–343.
- Steinmetz H, Herzog A, Schlaug G, Huang Y, Jäncke L (1995) Brain (a)symmetry in monozygotic twins. *Cereb Cortex* 5:296–300.
- Steinmetz H, Rademacher J, Huang Y, Hefter H, Zilles K, Thron A, Freund H-J (1989) Cerebral asymmetry: MR planimetry of the human planum temporale. *J Comput-Assist Tomogr* 13:996–1005.
- Steinmetz H, Rademacher J, Jäncke L, Huang Y, Thron A, Zilles K (1990) Total surface of temporoparietal intrasylvian cortex: diverging left-right asymmetries. *Brain Lang* 39:357–372.
- Steinmetz H, Volkman J, Jäncke L, Freund H-J (1991) Anatomical left-right asymmetry of language-related temporal cortex is different in left- and right-handers. *Ann Neurol* 29:315–319.
- Talairach J, Tournoux P (1988) Co-planar stereo atlas of the human brain. New York: Thieme.
- Tallal P, Miller S, Fitch R (1993) Neurobiological basis of speech: a case for the preeminence of temporal processing. *Ann NY Acad Sci* 682:27–47.
- Teszner D, Tzavaras A, Gruner J, Hecaen H (1972) L'asymétrie droit-gauche du planum temporale; à propos de l'étude anatomique de 100 cerveaux. *Rev Neurol* 126:444–449.
- Wada JA, Clarke R, Hamm A (1975) Cerebral hemispheric asymmetry in humans. *Arch Neurol* 32:239–246.
- Witelson SF, Paillie W (1973) Left hemisphere specialization for language in the newborn: neuroanatomical evidence of asymmetry. *Brain* 96:641–646.
- Witelson SF, Kigar DL (1992) Sylvian fissure morphology and asymmetry in men and women: bilateral differences in relation to handedness in men. *J Comp Neurol* 323:326–340.
- Witelson SF, Glezer II, Kigar DL (1995) Women have a greater density of neurons in the posterior temporal cortex. *J Neurosci* 15:3418–3428.